SIMULATION OF HOLLOW ELECTRON LENSES AS LHC BEAM HALO REDUCERS USING MERLIN*

H. Rafique[†], R. J. Barlow, University of Huddersfield, Huddersfield, UK
R. Appleby, S. Tygier, University of Manchester, Manchester, UK
R. Bruce, S. Redaelli, CERN, Geneva, Switzerland

Abstract

The Large Hadron Collider (LHC) and its High Luminosity (HL) upgrade foresee unprecedented stored beam energies of up to 700 MJ. The collimation system is responsible for cleaning the beam halo and is vital for successful machine operation. Hollow electron lenses (HELs) are being considered for the LHC, based on Tevatron designs and operational experience [1], for active halo control. HELs can be used as soft scraper devices, and may operate close to the beam core without undergoing damage [2]. We use the Merlin C++ accelerator libraries [3] to implement a HEL and examine the effect on the beam halo for various test scenarios.

INTRODUCTION

HELs are novel devices which generate and control a hollow beam of electrons through an accelerator beam pipe. By directing the accelerator beam through the HEL beam, one may achieve various effects via the electromagnetic interaction. At the Tevatron, electron lenses (ELs) have been used for beam beam compensation (solid electron beam) [4], removal of beam from the abort gap (solid electron beam) [5], and halo scraping (hollow electron beam) [2].

It was originally proposed [6] that ELs could be used for tune spreading, satellite bunch removal, and halo scraping in the LHC. When combined with a multi-stage collimation scheme such as that in the LHC, HELs become an enhancer, increasing the diffusion, and the impact parameter of halo particles hitting the primaries [7].

The benefits of a HEL in a collimation scheme are numerous; firstly the electron beam is well controlled, and has many operation modes that may enhance the collimation of halo particles. The HEL beam can intercept the machine beam at a greater insertion (lower σ) than a solid scraper, as there is no heat load to manage, and no effect on machine impedance. The HEL can be switched on and off whereas a solid scraper would need to be inserted, and though both require alignment setup, the HEL may be used on a turn by turn, or even bunch by bunch basis. This means that the HEL can be used to deplete the halo, so that beam losses are minimised in the case of a rapid orbit jitter or crab cavity failure in HL-LHC.

MERLIN HEL MODEL

Merlin makes a number of assumptions when modelling the HEL:

- Fringe fields are ignored.
- Multipole field components created by e^- beam asymmetries are ignored.
- The e^- beam is azimuthally symmetric.
- Edge effects from the HEL beam are ignored (transverse area of interest ≈ few mm, longitudinal ≈ few m).
- Only the active part of the HEL is considered (toroids and solenoids are ignored).
- The HEL is run such that the electrons travel in the same direction as the proton beam, so that the HEL kick given to a machine particle is focussing.

Implementation

For a HEL of length L, with electron beam current I, the kick for a particle at a transverse displacement r, neglecting the electron radial profile is given by Eq. 1 [8].

$$\theta_{max}(r) = \frac{1}{4\pi\epsilon_0 c^2} \frac{2LI(1 + \beta_e\beta_p)}{(B\rho)_p \beta_e\beta_p} \frac{1}{r} \qquad (1)$$

where β_e and β_p are the Lorentz β of the HEL electron beam, and machine proton beam respectively, and $(B\rho)_p$ is the proton beam rigidity.

Including the electron radial profile, the kick may be reduced, for example for a perfect HEL profile (uniform between R_{min} and R_{max} and axially symmetric) it is given by Eq. 2 [8].

$$\theta_{kick} = \begin{cases} 0, & r < R_{min} \\ \frac{r^2 - R_{min}^2}{R_{max}^2 - R_{min}^2}\theta_{max}, & R_{min} < r < R_{max} \\ \theta_{max}, & r > R_{max} \end{cases} \qquad (2)$$

Merlin contains both this perfect profile and a more realistic radial profile, based on the parameterisation of the measured beam profile [9]. The kicks for both profiles are shown in Fig. 1. R_{min} and R_{max} were set to 4 and 6.8 σ respectively.

In practice integration of a HEL into the LHC is non-trivial . The HEL is a superconducting device and therefore needs access to the LHC's high pressure He supply. As the HEL operates on one LHC beam, space between the two beam lines is required. Two candidate locations have been identified as RB-44 and RB-46, both in IR4, either side of the RF insertion [10]. Using Merlin, a HEL was implemented into the LHC lattice at RB-46. The optics parameters are shown in Table 1.

Operation Modes

The Merlin HollowElectronLensProcess offers 4 operation modes, similar to the HEL model in SixTrack [11].

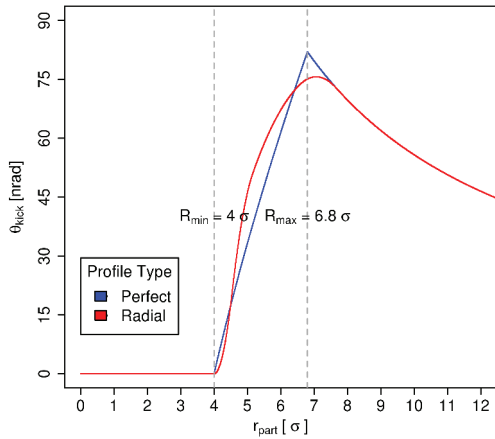**1: Circular and Linear Colliders**

T19 - Collimation

Figure 1: Kick for particle with displacement r for a perfect and measured (radial) HEL with $R_{min} = 4\sigma$ and $R_{max} = 6.8\sigma$.

Table 1: HEL Optics Parameters for Merlin Simulation

Parameter	Symbol [Unit]	Value
Lattice Position (end)	S [m]	10037
Amplitude Function	β_x [m]	181.745
Amplitude Function	β_y [m]	180.377
Beam Tilt Function	α_x [-]	0.315953
Beam Tilt Function	α_y [-]	-0.963648
Proton Beam Size	σ_x [μm]	291.998
Proton Beam Size	σ_y [μm]	290.897
Proton Beam Spread	σ'_x [μrad]	1.684922
Proton Beam Spread	σ'_y [μrad]	2.239659
Proton Kinetic Energy	E [TeV]	7
Electron Kinetic Energy	E [KeV]	5
Electron Beam Current	I [A]	1.2
Effective Length	L [m]	2

1. DC: HEL constantly at maximum, scraping relies on constructive production of resonances from machine and HEL non-linearities [12].
2. AC: HEL beam current is modulated to resonate with the betatron tune to drive the amplitude of particle oscillation [11].
3. Diffusive: HEL is randomly switched on/off on a turn by turn basis to enhance halo particle diffusion.
4. Turnskip: HEL is switched on every n turns, where n is an integer.

RESULTS

To observe the effects of a HEL on the LHC beam halo, single particle simulations were run for $5 \cdot 10^4$ turns. HEL radii are set to $R_{min} = 4\sigma_x$ and $R_{max} = 6.8\sigma_x$, and other parameters are as shown in Table 1. The HEL is oriented such that the LHC beam halo experiences a focussing kick if within or outside the HEL transverse profile. Particles with displacement $r < R_{min}$ are not perturbed as we assume

that the HEL beam is symmetric. Figure 2 shows the DC HEL driven particle oscillation for an on-momentum halo particle with a transverse displacement of $\approx 6\sigma_x$. Here the transverse angle of the particle is recorded at the start of the primary collimator TCP.C6L7.B1 ($s \approx 19790m$) for $5 \cdot 10^4$ turns. It is clear that the particle affected by the DC HEL is being focussed in the transverse x' plane, and thus x (which shows similar behaviour), as expected.
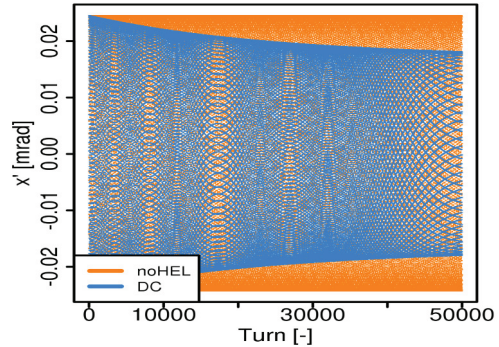

Figure 2: Particle motion in the LHC driven by a DC HEL (blue), compared to no HEL (orange), at the primary collimator ($s \approx 19790m$).

As the HEL kick operates on the transverse angle x' of the particle, the betatron tune of the particle is altered by an amount which depends on its amplitude. The number of betatron oscillations is expected to increase with a focussing HEL, this is observed in Fig. 3. Transverse particle oscillations, again measured immediately before the primary collimator, have been fitted to illustrate the positive shift in the betatron oscillation caused by the DC HEL. The HEL sinusoid has a smaller amplitude due to HEL induced focussing. We must note that when operating in DC mode, the tune will constantly be increased until the particle has displacement $r < R_{min}$.
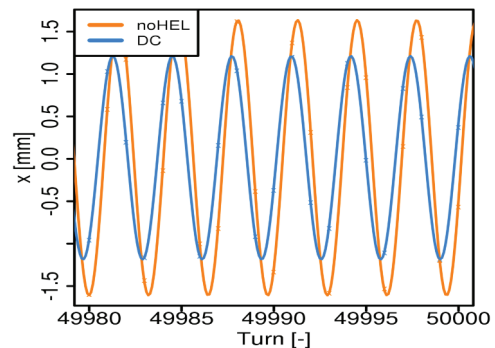

Figure 3: Particle transverse x position at the primary collimator ($s \approx 19790m$) in the LHC after 49980 turns. Position with (blue) and without (orange) a DC HEL has been fitted with a sinusoid to illustrate a tune shift of order $\approx +3 \cdot 10^{-4}$.

The LHC collimation system is concerned with the removal of halo particles from the LHC bunch, for machine protection amongst other things. Horizontal halo particles

are those that populate the outer edges of the proton bunch ellipse in xx' phase space. To observe the motion of halo particles, a phase space portrait was constructed for 7 particles, each with an initial displacement of 1-7 σ_x, each taken at a stable x'. This is shown in Fig. 4, where the effect of a DC HEL is compared with that of an AC HEL.

It is important to note that stable particles with $r < R_{min}$ will not enter the HEL beam but will traverse its hollow centre, and thus experience no kick. A halo particle with an initial $r < R_{min}$ may have a sufficiently large x' to hit the HEL (i.e. $r > R_{min}$), via normal betatron oscillation after a number of turns, and thus experience its effects.
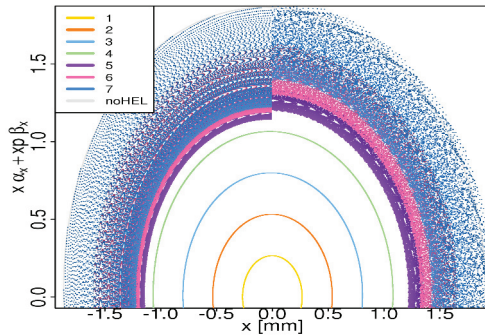

Figure 4: Normalised phase space portrait of LHC halo particles with initial displacement of $n\sigma_x$ ($n = \{1, 2, ..., 7\}$) for $5 \cdot 10^4$ turns. DC HEL for $x < 0$, AC for $x > 0$. HEL colour gradients are used, the darker colour indicating earlier turns, the case with no HEL is shown in grey, the legend shows initial particle displacement colours in σ_x.

It is clear from Fig. 4 that in the DC case halo particles are focussed towards the bunch core. The DC operation of the HEL as a scraper relies on resonances, which increase the particle displacement, thus driving it onto an aperture restriction such as a collimator. In the AC case we see that particles are not as focussed as in the DC case, in fact particle displacement increases at certain points. The AC HEL relies on coupling with the natural betatron oscillation of the particle in order to drive the displacement of high σ_x particles in this way. For particles with displacement $r < R_{min}$, we observe no change from stability as expected.

A single, primary collimator (TCP.C6L7.B1) was inserted horizontally, at a jaw opening of $6.2\sigma_x$, in order to simulate the HEL as a halo scraping device. As the kick given to a particle is of the order of nanoradians, and as observed in Fig. 4 the action of the HEL is dependent on operation mode and particle displacement, many turns are required to observe halo scraping. A uniformly populated bunch of horizontal halo particles between $4 - 6\sigma_x$ were simulated for $8 \cdot 10^4$ turns, and the initial and final distributions are shown in Fig. 5. In this case the HEL operates in Diffusive mode. As expected, the HEL is a more effective scraper at high particle displacement A_x.

Figure 6 shows that, for the initial distribution depicted in Fig. 5, when no HEL is present the bunch is stable and no particles impact upon the single collimator. When a HEL is
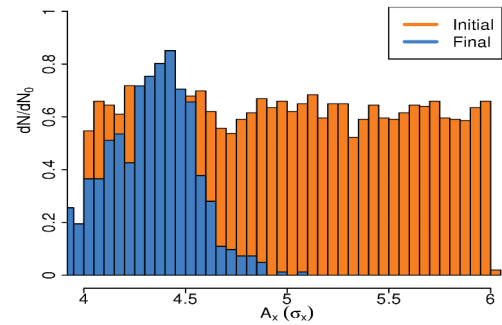

Figure 5: Normalised inital (blue) and final (orange) particle distributions for $8 \cdot 10^4$ turns in the LHC with a HEL operating in Diffusive mode.
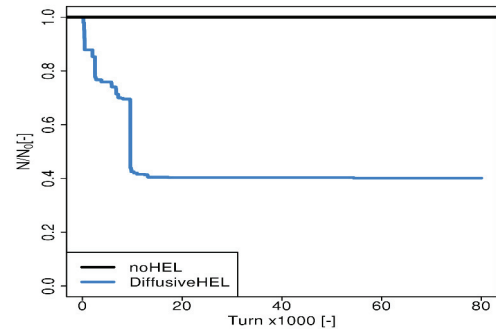

Figure 6: Normalised number of circulating particles for $8 \cdot 10^4$ turns in the LHC, with (blue) and without (black) a HEL operating in Diffusive mode.

operating in Diffusive mode however, $\approx 60\%$ of halo particles are kicked onto the primary collimator after $8 \cdot 10^4$ turns, around 2 seconds of machine time.

CONCLUSION

For the first time, a hollow electron lens has been implemented in Merlin, as a particle bunch process, and modelled for use in the LHC collimation system. In order to simulate the effect, and optimise the use, of a HEL as part of the multi stage LHC collimation system, large scale simulations are required. Preliminary tests have confirmed behaviour expected from experimental [9] and computational [8] experience. Focussing of the halo has been observed, together with the expected increase in the number of betatron oscillations (tune). It is clear that in DC mode, when not exciting a resonance, the HEL acts as a focussing device more than a scraper. In AC mode focussing is less apparent, and the natural betatron oscillations of high amplitude particles are driven, increasing particle displacement. As expected the HEL is most effective as a scraper at particle displacements near the maximum radius R_{max} of the electron beam. Simulations indicate that in Diffusive mode, the HEL may be used to clean the LHC beam halo in a few seconds.

REFERENCES

[1] V. Shiltsev, *et al*., "Electron Lenses for Particle Collimation in LHC", FERMILAB-CONF-07-698-APC.

[2] G. Stancari *et al*., Phys. Rev. Lett. 107, 084802 (2011).

[3] http://merlin-pt.sourceforge.net/

[4] V. Shiltsev *et al*., Phys. Rev. Lett. 99, 244801 (2007).

[5] Zhang *et al*., Phys. Rev. ST Accel. Beams 11, 051002 (2008).

[6] V. Shiltsev, Proc. BEAM06, Yellow Report CERN-2007-002.

[7] J. Claiborne Smith *et al*., "Prospects for Integrating a Hollow Electron Lens into the LHC Collimation System", Proc. PAC09, Canada, 2009.

[8] V. Previtali *et al*., "Numerical Simulations of a Hollow Electron Lens as a Scraping Device for the LHC", IPAC13, China, 2013.

[9] V. Moens, "Experimental and Numerical Studies on the Proposed Application of Hollow Electron Beam Collimation for the LHC at CERN", CERN-THESIS-2013-126.

[10] G. Stancari *et al*., "Conceptual Design of Hollow Electron Lenses for Beam Halo Control in the Large Hadron Collider", FERMILAB-TM-2572-APC.

[11] V. Previtali *et al*., "Hollow Electron Lens Simulations for the SPS", IPAC13, China, 2013.

[12] V. Previatli *et al*., "Numerical Simulations of Transverse Beam Diffusion Enhancement by the use of Electron Lens in the Tevatron Collider", Conf. Proc. C 1205201, 1113 (2012).